Pheromone synthesis in a biomicroreactor coated with anti-adsorption polyelectrolyte multilayer

Nikolay Dimov,[1,a)] Lourdes Muñoz,[2] Gerard Carot-Sans,[2]
Michel L. P. M. Verhoeven,[1] Wojciech P. Bula,[1] Gülistan Kocer,[1]
Angel Guerrero,[2] and Han J. G. E. Gardeniers[1]
[1]*Mesoscale Chemical Systems, MESA+ Institute for Nanotechnology, University of Twente, 7500 AE Enschede, The Netherlands*
[2]*Department of Biological Chemistry and Molecular Modeling (IQAC-CSIC), 08034 Barcelona, Spain*

(Received 7 April 2011; accepted 13 June 2011; published online 19 July 2011)

To prepare a biosynthetic module in an infochemical communication project, we designed a silicon/glass microreactor with anti-adsorption polyelectrolyte multilayer coating and immobilized alcohol acetyl transferase (*atf*), one of the key biosynthetic enzymes of the pheromone of *Spodoptera littoralis*, on agarose beads inside. The system reproduces the last step of the biosynthesis in which the precursor diene alcohol (*Z,E*)-9,11-tetradecadienol is transformed into the major component (*Z,E*)-9,11-tetradecadienyl acetate. The scope of this study was to analyze and implement a multilayer, anti-adsorption coating based on layer-by-layer deposition of polyethylenimine/dextransulfate sodium salt (PEI/DSS). The multilayers were composed of two PEI with molecular weights 750 and 1.2 kDa at *p*H 9.2 or 6.0. Growth, morphology, and stability of the layers were analyzed by ellipsometry and atomic force microscopy (AFM). The anti-adsorption functionality of the multilayer inside the microreactor was validated. The activity of His_6-(*atf*) was measured by gas chromatography coupled to mass spectrometer (GC-MS). © *2011 American Institute of Physics*. [doi:10.1063/1.3608138]

I. INTRODUCTION

Insects communicate with their con-specifics using complex blends of volatile chemicals called pheromones. The pheromone communication system consists of the release of specific chemical blends, generally by the females, to the environment that are then detected by a very sensitive olfactory system of the males. These chemical blends are biosynthesized in a pheromone gland in most cases from fatty acids by pheromone specific enzymes. The biosynthetic pathways of the sex pheromone of the moth *Spodoptera littoralis*[1] was taken as a starting point for the development of a chemical communication system to mimic the generation and reception of a chemical signal.[2] One of the biosynthetic modules is an enzymatic microreactor system to perform the final biosynthetic step in the production of the major component of the pheromone, (*Z,E*)-9,11-tetradecadienyl acetate.[1] In the future, such modules will be hierarchically integrated to establish a chemoemitter for infochemical communication.

The last step in the biosynthesis of all components of the pheromone blend of *S. littoralis* consists of the transfer of an acetyl group from acetyl-CoA to the precursor alcohol. This reaction is catalyzed in the moth by an alcohol acetyl transferase. However, due to the absence of a known acetyl transferase in *S. littoralis*, we selected an orthologue (a wax ester synthase, *atf*) to perform the same biochemical reaction (Fig. 1). The *atf* esterifies aliphatic alcohols with carbon chains longer than 6 into the corresponding acetates.[3] To exploit this enzymatic reaction in a microreactor module, a route was sought to immobilize the enzyme in a microreactor

[a)]Author to whom correspondence should be addressed. Electronic mail: n.g.dimov@utwente.nl.

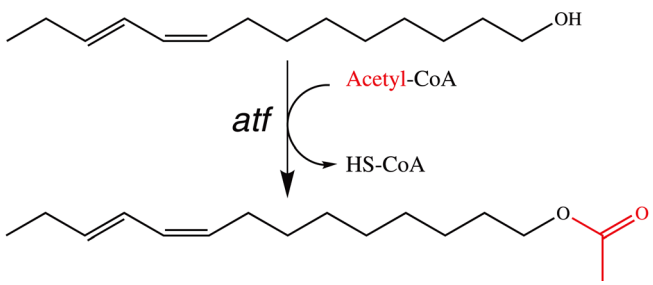

FIG. 1. Bioconversion catalyzed by an alcohol acetyl transferase (a wax ester synthase, *atf*, in this paper). In the presence of acetyl-CoA *atf* transforms the (*Z,E*)-9,11-tetradecadienol, the pheromone precursor, into (*Z,E*)-9,11-tetradecadienyl acetate, the pheromone product.

compartment. Several of such compartments, containing different biosynthetic enzymes, may then be connected by an integrated microfluidic network (see e.g., Ref. 4) in order to mimic the complete biosynthetic pathway. Several methods to immobilize enzymes in a microfluidic environment have been described in the literature,[5–8] and for simplicity, we followed a similar procedure to that reported by Seong *et al.*[9] This involved immobilization of the enzyme on microbeads and package of the beads into a microfluidic chip, through which a flow of the substrate solution was passed to produce the expected product at the outlet.

Preliminary experiments with such a construct showed that the compounds of our interest were prone to adsorb on the surface of the silicon/glass microreactor. Previous fundamental studies have proved that adsorption on silicon surfaces (with a native oxide) occurs on silanol groups.[10,11] Building a polyelectrolyte multilayer (PEM) on these negatively charged groups may mask the charges and prevent adsorption. Deposition of PEM was implemented using a layer-by-layer (lbl) technique, suggested by Iler[12] and later developed by Decher.[13] The polyelectrolyte system explored here was polyethylenimine/dextransulfate sodium salt (PEI/DSS). A similar approach was adopted by Kim and Urban as a basis for thromboresistant thin films on polyvinyl chloride.[14] The polyelectrolyte modification of microreactor surfaces is a versatile method in terms of layer optimization which allows fine tailoring of interfacial properties of glass, silicon, and poly(dimethylsiloxane) (PDMS).[15–17] During the last two decades, research has been performed on polyelectrolyte stability,[18] growth regimes,[19,20] and interaction with proteins.[21,22] Additionally, specific knowledge on PEI charge density,[23,24] adsorption behavior,[25,26] and dynamics of protein interactions at interfaces[27] provide us solid ground for further exploration and implementation of the PEI/DSS couple in a biomicroreactor.

Foregoing literature describes the adsorption of PEI on silica[19,25,26] and the PEI coupling to epoxysilane for attachment of antibodies;[28] however, the PEI/DSS polyelectrolyte couple has not been studied in details for deposition on silanized silicon surfaces. Thus, it is important to characterize the layer formation and thickness on the silanized substrate under various conditions and to compare with their non-silanized counterparts before application in a microreactor.

II. MATERIALS AND METHODS

Branched polyethyleneimine (PEI) 50% (wt.) solution with molecular weight 750 kDa and PEI with molecular weight 1.2 kDa as polycations and DSS from *Leuconostoc* spp. as polyanion with molecular weight 500 kDa were used in the lbl deposition. The cross linking reagent, crotonaldehyde, sodium cyanoborohydride ($NaCNBH_3$), sodium chloride (NaCl), acetate, MES monohydrate and borate buffers, dodecyl acetate (97%), toluene (anhydrous GC grade), *N,N*-dimethyl-formamide (DMF), dimethyl sulfoxide (DMSO, GC grade), glycerol, acetyl coenzyme A sodium salt (acetyl-CoA), Trizma HCl (Tris-Cl), hydrogen peroxide (H_2O_2, 30%), (3-glycidoxypropyl)trimethoxysilane (97%, GC grade), and sulfuric acid (H_2SO_4, 98%) were purchased from Sigma-Aldrich (Chemie BV, Germany) and used without further modification. The (*Z,E*)-9,11-tetradecadienyl acetate was purchased from Bedoukian (Danbury, USA).

The agarose beads were part of HisBand purification kit from Novagen (Darmstad, Germany). One side polished 4 in. Si{100} wafers were obtained from Okmetic (Vantaa, Finland), 4 in. borofloat glass wafers were purchased from Schott AG (Benelux, The Netherlands).

A. Surface activation before layer deposition

Characterization of lbl deposition was conducted on 7×7 mm^2 pieces diced from the silicon wafer (Disco DAD-321, Tokyo, Japan). Prior to layer deposition, the silicon pieces were activated with piranha solution (H_2SO_4 (98%):H_2O_2 (30%) 3:1) for 25 min. (Attention: Piranha is a strong oxidizing agent!) The abundance of hydroxyl radicals from piranha opens the siloxane bonds on the Si/SiO_2 surface to form silanols. Surfaces were washed for 25 min with copious amount of Milli-Q water (Millipore, Billerica, USA), dried in N_2 flow and on a hotplate in air at 100 °C for 5 min.

B. Polyelectrolyte layer-by-layer deposition

1. Non-anchored layer

In our study, direct deposition of non-anchored PEM on the activated wafer surfaces was performed by lbl adsorption,[13] an electrostatically driven sequential deposition of polyelectrolytes from water solutions. Initial experimental conditions for the PEM generation were chosen according to Kim and Urban.[14] Two variants of PEI, with molecular weight 1.2 kDa and 750 kDa, were used as polycations during the lbl deposition. For each molecular weight 0.01% (wt.), PEI aqueous solutions were prepared in 10 mM MES buffer at *p*H 6 and 10 mM borate buffer at *p*H 9.2. Crotonaldehyde (4.1 μM) was added and the salt concentration was adjusted to 1.7 mM NaCl. Time of incubation in the PEI solution was 10 min at room temperature. The loosely bound PEI molecules were removed with sufficient amounts of Milli-Q water.

The Si pieces were transferred consecutively into Eppendorf tubes containing 0.4% (wt.) DSS in 10 mM acetate buffer, *p*H 3.8, with 1.7 mM NaCl and incubated for 10 min at room temperature. Non-adsorbed DSS molecules were discarded by washing with Milli-Q.

An odd number of layers were deposited alternating PEI with DSS, thus terminating the build-up with positively charged PEI.

2. Anchored layer

Anchored PEM, via (3-glycidoxypropyl)trimethoxy silane, was obtained following a slightly modified protocol from the originally reported covalent attachment on silicon beads.[29] Activated, dry, Si pieces were incubated in 1.5% (3-glycidoxypropyl)trimethoxy silane solution in anhydrous toluene for 2 h and then rinsed with DMF. Coupling of the amino group to the epoxy was done overnight using 0.01% (wt.) PEI (molecular weight 1.2 kDa or 750 kDa) in DMF. The *p*H values were maintained with 10 mM MES, *p*H 6, or 10 mM borate buffer, *p*H 9.2. The Si pieces were rinsed with Milli-Q water. The processing continued for an odd number of layers as the direct deposition lbl described above, terminating with PEI as target molecule because of its positively charged amino groups.

3. Reduction of the Schiff bases

To complete the process and to obtain stable cross linking, a 10 mM solution of $NaCNBH_3$ in 10 mM acetate buffer, *p*H 3.8, was applied to the surface for 1 h at room temperature. During this step, the Schiff bases were reduced. Surfaces were rinsed with water and dried overnight at 30 °C before characterization.

C. Characterization of the polyelectrolyte layers on Si surface

Surface morphologies and step heights were studied with a commercial atomic force microscope (Dimension Icon, Bruker, Germany) equipped with a Nanoscope V controller. All scans were obtained in non-contact mode using rectangular silicon cantilevers (NCH, NanoWorld,

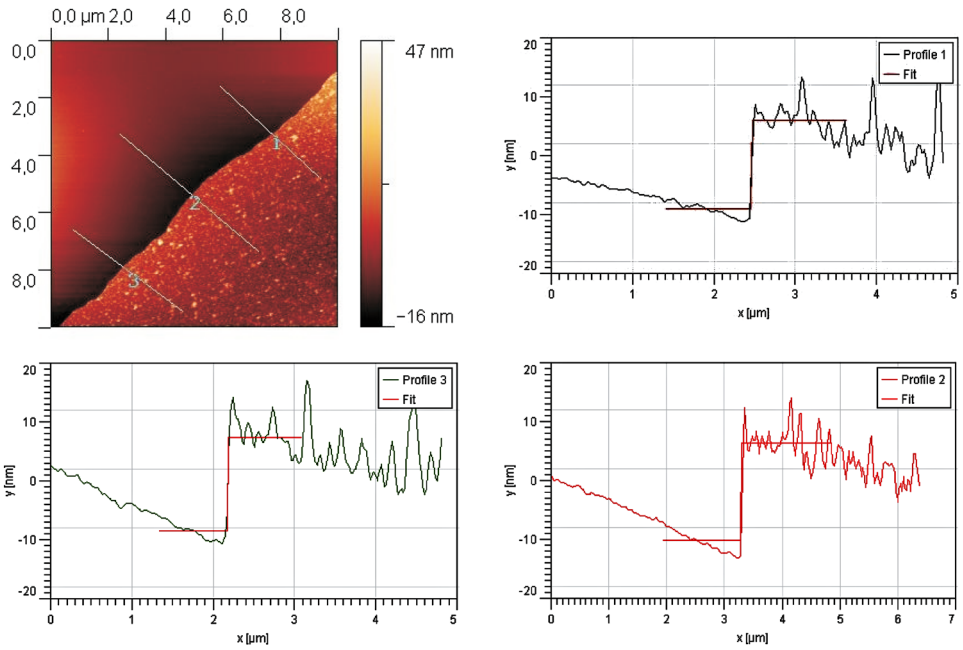

FIG. 2. Height of step measurement. Three cross sections were set in random positions on the AFM scan across the scratch/coating interface and a model was fit measuring the step heights.

Switzerland) with a force constant of 42 N/m. Roughness of the surfaces was determined for a constant scan area of 1×1 μm on dry samples. The raw data were processed and visualized with GWYDDION (version 2.19), an open source software.

The scans for the step measurements were conducted after scratching away part of the coating with a scalpel. Then heights were obtained from those scans by fitting a step-height (GWYDDION) to the interface between scratch and coating. For each surface modification, the mean height value and standard deviation were calculated from three cross sections, illustrated in Fig. 2.

The thickness of dry polymer layers was determined by ellipsometry on the Si pieces after each layer of the PEM deposition process. Angles Ψ and Δ were measured with a VASE (J. A. Woollam Co., Inc, Lincoln, USA) ellipsometer at three incident angles, 65°, 70°, 75°, using the wavelength (λ) from 250 to 1250 nm. The number of samples was duplicated in order to evaluate the reproducibility of lbl deposition. Thickness and refractive index of the native oxide layer on bare Si pieces were obtained by using the WVASE32 modeling software for the measured Ψ and Δ in the beginning of each experimental series. The mean layer thickness was calculated from the three incident angles data, fitted by the two layer Cauchy mathematical model.

Stability of the coatings was evaluated by comparison of thicknesses before and after incubation in working conditions. The initial layer thicknesses were ellipsometrically measured, two points from each sample, then the samples were left in 10 mM Tris-Cl (*p*H 7.3) with 10% glycerol at 30 °C for a week. Samples were dried and the measurements were repeated.

D. Fabrication of the silicon/glass microreactor

Fabrication of the silicon-glass microreactor followed well established techniques.[30] The 200 μm deep channel was etched with straight walls into the silicon wafer after 10 min "Bosch" directed reactive ion etching (B-UNIFORM recipe, Adixen AMS100SE, Alcatel, France). The fluorides, formed during Bosch processing, were striped first with oxygen plasma for 10 min (500 W) followed by 15 min at 800 °C. Resulting SiO_2 was etched for 2 min in 50% HF. A Borofloat wafer was cleaned, spin dried, and anodically bonded (EV 501 Bonding Station, EV Group, Austria) to the clean, dry Si wafer.

E. Adsorption of (*Z*,*E*)-9,11-tetradecadienol and (*Z*,*E*)-9,11-tetradecadienyl acetate inside the silicon/glass microreactor

Reaction buffer with predefined concentrations of substrate and product were flown through the microreactor at a rate of 10 μl/min. The non-coated microreactor with non-coated syringe and capillary was compared with the microsystem (microreactor and capillaries) coated with high molecular weight (HMW) PEI/DSS (*p*H 9.2/3.8) in the adsorption experiment. Collected fractions at the outlet were extracted with hexane and analyzed by gas chromatography coupled to mass spectrometer (GC-MS) (ThermoFisher Sci., Madrid, Spain).

F. Determination of His_6-EGFP adsorption inside a silicon/glass microreactor

Standard dilutions were prepared from a stock solution of 40 μM enhanced green fluorescent protein with Histidine tag (His_6-EGFP) in 10 mM Tris-Cl containing 10% glycerol. Fifty microliters of the stock solution was transferred into an Eppendorf tube with 50 μl of 10 mM Tris-Cl, 10% glycerol to result in 20 μM concentration. By repeating this process, standard solutions of 10, 5, 2.5, 1.25, and 0.625 μM were obtained. Non-coated microreactor was filled with the last standard dilution, a fluorescent image was acquired at magnification $\times$20 with 4 s exposure time using a microscope with external light source (Leica AF6000 with EL6000, Leica microsystems, Germany), and the microreactor was flushed with water. The process was repeated with the next dilution sample (1.25 μM) and so on. The obtained fluorescent images were converted (MATLAB 2008, The MathWorks, USA) to 8-bit gray scale images and the average of the pixel intensity was calculated for each image. The collected data points were plotted versus the protein concentration to generate the calibration curve shown in Fig. 3.

For the adsorption measurement 20 μM His_6-EGFP solution was inserted in an anchored HMW PEI/DSS (*p*H 9.2/3.8) coated microreactor and incubated for 30 min at room temperature. An image of the microreactor was acquired to evaluate fluorescence of the protein. The biomicroreactor was shortly rinsed with buffer and another image was acquired. Measurements were triplicated. The amount of adsorbed His_6-EGFP was determined by using the calculated intensity from these images and the already generated calibration curve.

G. Expression and purification of His_6-atf

The construction pET23a::His_6atf was transformed into *Escherichia coli* (strain Rosetta (DE3)pLys) and protein was expressed according to the procedure described by Steinbüchel *et al.*[3] Next the overexpressed *atf* was purified from the crude extract by metal affinity chromatography (Novagen), followed by membrane dialysis (MWCO 68000, 6.4 mm diameter; Spectrumlabs) to remove the imidazole used during the chromatographic elution.

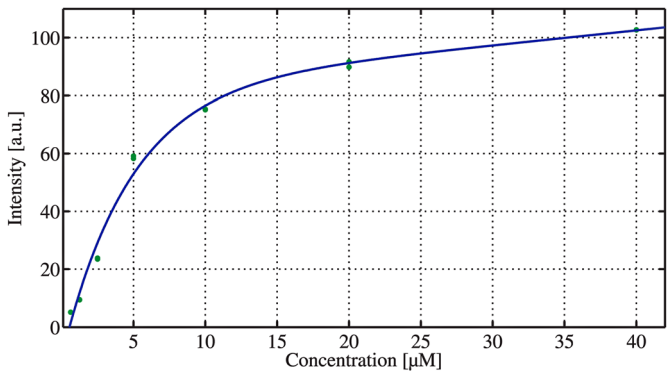

FIG. 3. Calibration curve imaging the His_6-EGFP content versus the fluorescence intensity measured inside a microreactor. Fluorescent images were acquired in duplicate and concentrations were plotted against their intensity values, the data were fitted to an exponential curve.

H. Immobilization and activity assay of the His_6-atf inside the microreactor

In total a five layer structure was anchored via (3-glycidoxypropyl)trimethoxy silane inside a microreactor and capillaries, following the protocol described above and using HMW PEI/DSS (*p*H 9.2/3.8) for 10 min deposition time in a stopped flow mode. Then, 100 μl of solution containing Nitrilotriacetic acid (NTA) functionalised agarose beads was introduced into the microreactor. The beads were prevented from leakage by adjusting the gap between the capillary and microreactor outlet smaller than the smallest measured bead diameter approximately 30 μm. Further, conditioning of the packed agarose beads was performed in accordance with the Novagen protocol for protein purification.

A solution of 10 μg His_6-*atf* in 10 mM Tris-Cl, *p*H 7.3, with 10% glycerol was prepared. The solution was manually injected into the microreactor and incubated for 30 min. The collected fraction was re-injected, and incubation was repeated till the total incubation time was 2 h. The enzyme was kept on ice during incubation. The biomicroreactor was thoroughly washed with buffer using a syringe pump (PHD 2000 Programmable, HARVARD apparatus, UK) at 10 μl/min for 15 min.

For the activity assay, the reaction buffer contained 10 mM Tris-Cl (*p*H 7.3) with 10% glycerol, 250 μM acetyl-CoA, 320 μM (*Z,E*)-9,11-tetradecadienol, and 4% DMSO. The DMSO was used as solvent to prepare the stock solution of 8 mM (*Z,E*)-9,11-tetradecadienol. The reaction buffer was run through the system at 10 μl/min using the syringe pump. Fractions were collected from the outlet of the biomicroreactor in sealed glass vials. A batch reaction experiment was set in parallel under the same conditions.

I. Hexane extraction and measurement of pheromone concentration by GC-MS

Extraction of the organic material from the aqueous phase was done with hexane. Dodecyl acetate (0.2 ml of a 0.3 μg/ml solution) was added to the extract, vortexed for 1 min. The samples were frozen in dry ice, the organic fractions were taken out with a Pasteur pipette, concentrated to ca. 20 μl and analyzed by GC-MS on a HP-5MS column (Agilent Technologies, Madrid, Spain). This step was done in duplicate. Injector and detector (FID) temperature were set to 280 °C. The oven temperature was initially set at 80 °C and increased at 3 °C/min until 280 °C, which was held for 10 min. The injections were done in splitless mode at 60 ml/min and a splitless time of 0.6 min. Helium was used as a carrier gas at a flow rate 1.3 ml/min.

III. RESULTS AND DISCUSSION

A. Characterization of polyelectrolyte multilayer thickness and morphology

We studied the effect of *p*H and MW on the thickness of one, three, and five layers on flat silicon silanized surfaces and compared the results with those of non-silanized surfaces. The results obtained for both silanized and non-silanized surfaces (Figs. 4(a) and 4(b)) showed that the thickness of PEM deposited at alkaline *p*H is larger than the thickness of the layers deposited at acid *p*H. The same general trend can be observed irrespective of the number of layers. These results can be explained by the adsorption energy, solvency, and electrostatic interactions.[31] The latter, also known as Coulombic interactions, can be influenced by the surface and polymer charge density, as well as the ionic strength of the solution due to the influence of *p*H on the surface charge density, and to the dissociation of amino groups in the PEI molecules. For instance, in the case of PEI from Fig. 4(a), the anchoring layer on the surface screens the negatively charged silanols and shifts the electrostatic interaction towards a covalent bond formation between an amino and an epoxy group. In comparison, on the non-silanized surfaces (Fig. 4(b)), the PEI layer is rather thin in all four experimental variations. This is due to the fact that electrostatic forces govern the deposition and once the charges on the Si surface are compensated, no further growth takes place.

In the case of anchored PEI/(DSS/PEI)×2, illustrated in Fig. 4(a), the buildup reaches 21.9 ± 0.2 nm for the HMW at *p*H 9.2 because the electrostatic interaction is restored with the lbl deposition. Moreover, low molecular weight (LMW) at the same *p*H is approximately 3 nm

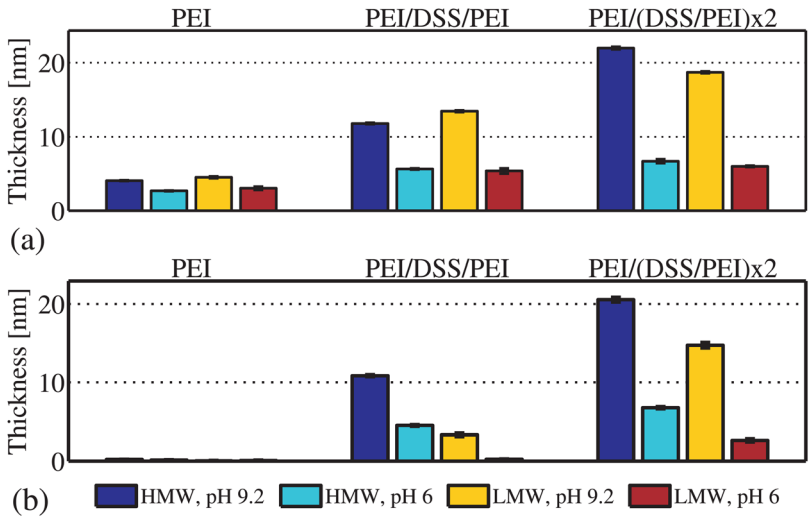

FIG. 4. Effects of *p*H and molecular weight of PEI on layer thickness after 10 min incubation. In total, five polyelectrolyte layers were generated on planar (a) silanized with (3-glycidoxypropyl)trimethoxy silane and (b) non-silanized silicon surfaces using PEI with HMW = 750 kDa or LMW = 1.2 kDa.

thinner. Another group is formed by the HMW at *p*H 6 with 6.7 ± 0.3 nm thickness and LMW at *p*H 6 for which the thickness was 6.0 ± 0.1 nm. Strong evidence of the *p*H influence on the PEI/DSS growth was obtained by AFM step measurement. The results are consistent, within the error, to the experimental values from the ellipsometry, Table I.

Thus, *p*H influences significantly the thickness, especially with higher layer number, and therefore is a suitable control parameter for layer thickness.

Another parameter that influences the deposition of PEM is the time of adsorption. The most suitable method for this investigation was to utilize non-silanized surfaces because of the marginal differences between the two types of substrate in terms of growth, especially for high layer numbers. Therefore, we measured the non-silanized samples with 5, 10, 15, and 20 min deposition time between two consecutive layers (Fig. 5(a)).

Looking at the mean thickness for five layers, all coatings are within 18 to 21 nm. A similar situation was observed for the mean values measured from the four layer structures: in the same interval of deposition times the thickness values were in the range of 10 to 14 nm. Based on these results, it can be stated that the deposition time between two consecutive layers does not influence the deposition process of PEI/DSS multilayer, because the difference in thickness between 5 and 20 min time of deposition is relatively small within the same number of layers. The finding is in agreement with the work of Müller and Paulik[27] on PEI/PAC and the earlier study by Cohen-Stuart *et al.*[18] The former used ATR-FTIR to study the kinetics and showed a steep ascent for less than 5 min deposition time, which is outside our region of investigation; however for longer deposition times, the thickness increased slightly. Therefore, any of the times from the studied interval (5 to 20 min) could be implied for coating a microsystem and the resulting PEI/DSS thickness would not vary strongly between the same number of layers generated at different times of deposition.

TABLE I. Thickness of PEMs deposited on silanized silicon surfaces. From the generated AFM scans, the height of step (mean values ± SD) is presented.

	PEI	PEI/DSS/PEI	PEI/(PEI/DSS) × 2
HMW, *p*H 9.2	3.9 ± 2.1	15.4 ± 3.5	24.4 ± 4.5
HMW, *p*H 6	3.2 ± 1.2	6.0 ± 1.0	6.7 ± 1.4
LMW, *p*H 9.2	5.3 ± 1.6	12.9 ± 1.4	19.3 ± 2.3
LMW, *p*H 6	1.9 ± 1.5	7.3 ± 1.8	7.8 ± 0.6

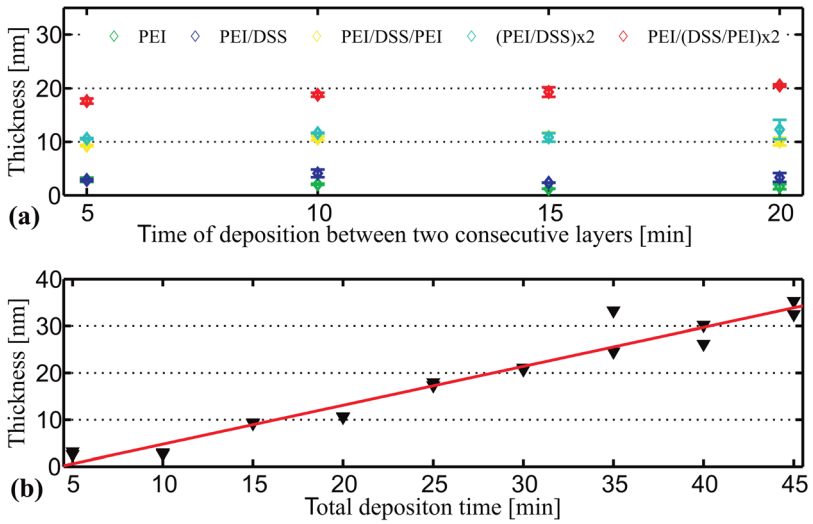

FIG. 5. Layer thickness versus time of deposition. Five single PE layers were generated starting with HMW PEI, *p*H 9.2, and alternating with DSS, *p*H 3.8. The thicknesses were measured in duplicate by Ellipsometry, one point per sample, after each deposition step. Plotted were (a) the mean values of thicknesses and standard deviations for increasing times of deposition between two consecutive layers from 5 min to 20 min; (b) experimental data (symbols) and fitted function correlating the thickness to the total deposition time, $R^2 = 0.95$.

The thickness growth of the PEI/DSS (*p*H 9.2/3.8) has linear behavior with the total deposition time. This trend, which is attributed to the lack of diffusion between consecutive layers is shown in Fig. 5(b) for 5 min deposition between two single layers. The results are consistent with the findings by Bieker and Schönhoff,[20] although these authors applied a different polyelectrolyte couple. By using the established linear growth pattern, it is possible to adjust the thickness of the PEI terminated multilayer coating for more than five layers.

AFM scans, illustrated in Fig. 6, show the influence of the number of layers on the morphology and roughness (RMS) of the HMW PEI/DSS coating (*p*H 9.2/3.8). The coverage of the first layer (a) is already sufficient as the layer appears homogeneous with a granular structured coating. The roughness of this layer is the lowest of all four layers, RMS = 0.41 nm. In the second and third layers, the granular structures grow in size which results in increase in roughness from 1.34 nm (b) to 1.66 nm (c). Although the RMS values differ by 0.22 nm, it can be seen that bulky structures start to form on the surface of the three layer coating (c). Roughness reaches a value of 5.55 nm for layer (d) whilst the grain structure does not alter in comparison to the third layer (c). The influence of time on roughness, for the PEI/PAC couple, has been documented in previous research.[27] In their work, the authors presumed that an increase in adsorption time would lead to an increase in RMS. In contrast, the current findings on the PEI/DSS couple allow us to assume that roughness increase is dependent on the number of layers even for constant time of deposition.

The PEMs have implicit porous structure, as observed in Fig. 6. On the first two surfaces, such porosity might result in non-protected silanol groups and consecutive pheromone adsorption because of poor layer coverage and low thickness. Therefore, they were considered unsuitable for modifying the silicon/glass microreactor. The coverage of both layers (c) and (d) would be sufficient to prevent adsorption.

B. Layer stability in working conditions

The results from the measurements are summarized in Figs. 7(a) and 7(b), from which it becomes clear that there is no depletion of the surface coating after 1 week. The coatings have no decrease in thickness before and after the incubation period for both silanized and non-silanized samples. For the LMW layer generated at *p*H 9.2, an increase of the thickness was observed, in the authors' opinion, due to residual water on the sample. Nevertheless, it can be

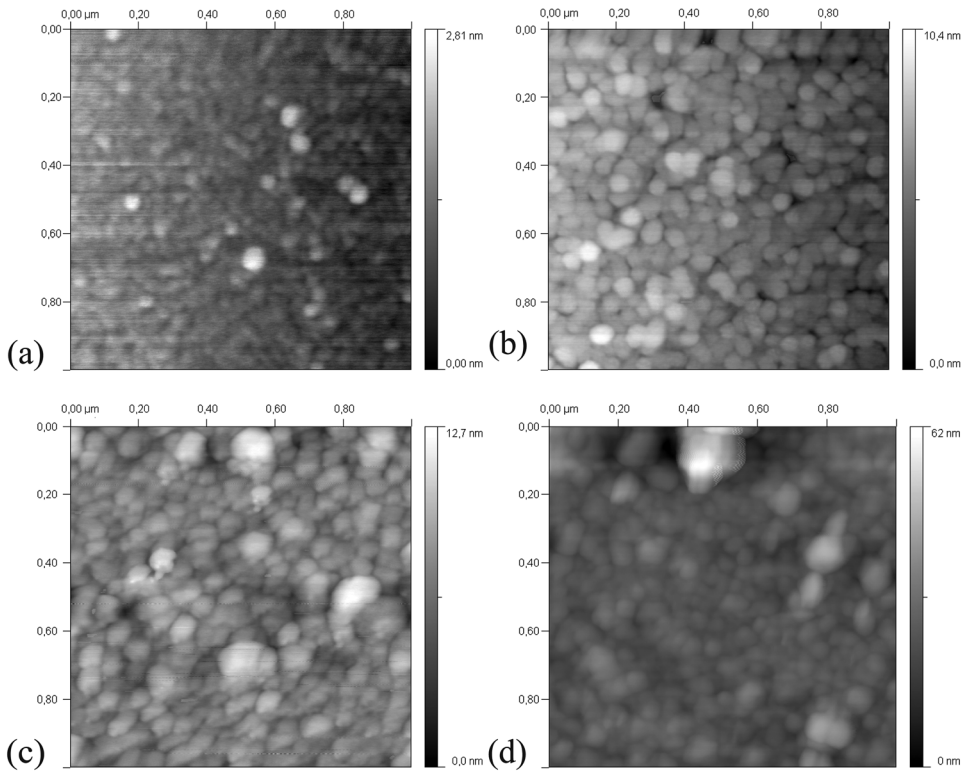

FIG. 6. AFM scans representing the surface morphology of polyelectrolyte coating, deposited at 10 min of incubation, on silinated silicon substrate: (a) one layer (PEI), RMS = 0.41 nm; (b) two layers (PEI/DSS), RMS = 1.34 nm; (c) three layers (PEI/DSS/PEI), RMS = 1.66 nm; (d) five layers (PEI/(DSS/PEI)×2), RMS = 5.55 nm.

stated that, in static conditions, without flow, PEM stability is not dependent on the anchoring layer. The PEI/DSS multilayer is stable and suitable for application in a biomicroreactor for pheromone synthesis.

C. Chemical and biological inertness of PEI terminated coating inside a microreactor

The recovered amounts of dienol and acetate for three different experimental conditions are summarized in Fig. 8 as percentage of the initial concentration. The recovered substrate (*Z,E*)-9,11-tetradecadienol from the syringe and capillary was approximately 38%. The recovered amount was lower in the non-treated system (12%), whereas for the one coated with the five single layers, the recovered amount of alcohol increased to 85%. Recovery of the product (*Z,E*)-9,11-tetradienyl acetate was lower in the three cases, amounting to 4% in the non-coated system, 18% for the syringe and capillary, and 60% for the PEM coated microsystem. These data confirm the efficiency of the PEM as anti-adsorption layer (ca. 20× the recovered amount of substrate and product in comparison to the non-coated system).

The substrate recovery is close to the initial concentration. Overall, loss of product may be due to the polar nature of the acetate functional group of the pheromone, which is retained possibly due to interactions with the PEI terminal layer. The exact mechanism of adsorption for the (*Z,E*)-9,11-tetradecadienol and (*Z,E*)-9,11-tetradienyl acetate on the weak PEM coating is still not clear. In the authors' opinion, due to the porosity of the PEM coating there might be regions with active negative charges either from the Si surface or the DSS. Plausibly, the swelling of the PEM would enhance the effect, by exposing charged sites on the surface. Equally valid, if the charge on the terminal PEI layer approaches zero, the repulsion from the surface would diminish and adsorption would eventually take place because of weak interactions. The zero surface charge could be a result of the charge overcompensation, which is assumed to be

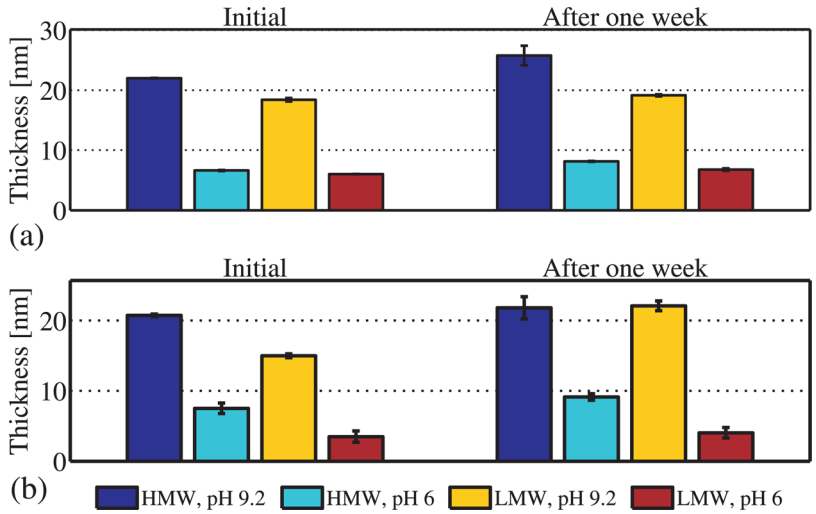

FIG. 7. Effects of incubation for 1 week in the specified solution. Five PE layers were deposited on, (a) silanized with (3-glycidoxypropyl)trimethoxy silane and (b) non-silanized, silicon surfaces using PEI with HMW = 750 kDa or LMW = 1.2 kDa.

the driving force for PEM formation during the lbl deposition. Additionally, the ionic strength of the solution could also lead to zero charge, according to the Derjaguin, Landau, Verwey, and Overbeek[33,34] theory (DVLO). Nonetheless, the recovered amount for the (*Z,E*)-9,11-tetradienyl acetate is 20 times higher from the coated microsystem than from its non-coated counterpart. According to these results, the enzymatic reaction should be achievable in a PEM coated microsystem.

Next, the effect of the PEM coating on adsorption of protein was studied. The retained His_6-EGFP on the walls of the microchannel was determined, and amounted to less than 0.2 μM. Even though a direct comparison between the adsorption behavior of His_6-EGFP and His_6-*atf* would be futile, since these two proteins have different amino acid sequences and structure, we can infer it indirectly. The native isoelectric point of His_6-EGFP proteins is in the range of 5–6.2,[32] which will result in an overall negative charge for His_6-EGFP at the immobilization conditions (*p*H 7.3). On the other hand, *atf* is positively charged at *p*H 7.3.[35] Therefore, if His_6-

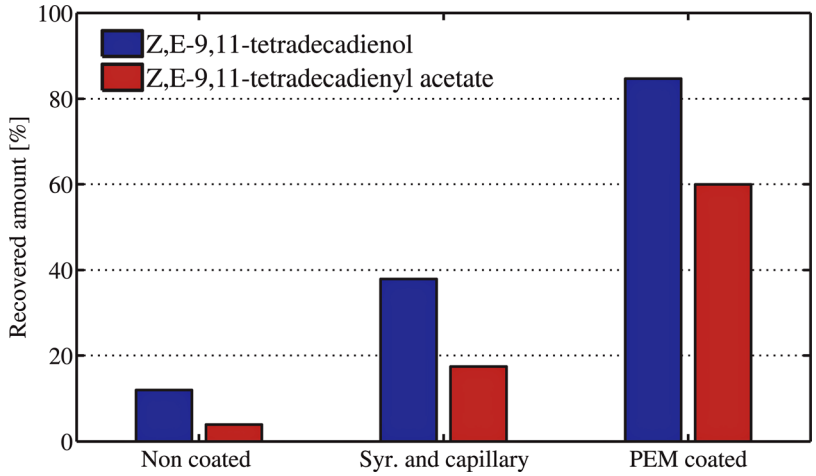

FIG. 8. Amount of (*Z,E*)-9,11-tetradecadienol and (*Z,E*)-9,11-tetradienyl acetate recovered after passing through a non-coated microreactor, non-coated syringe and capillary, and microreactor and capillary coated with PEM.

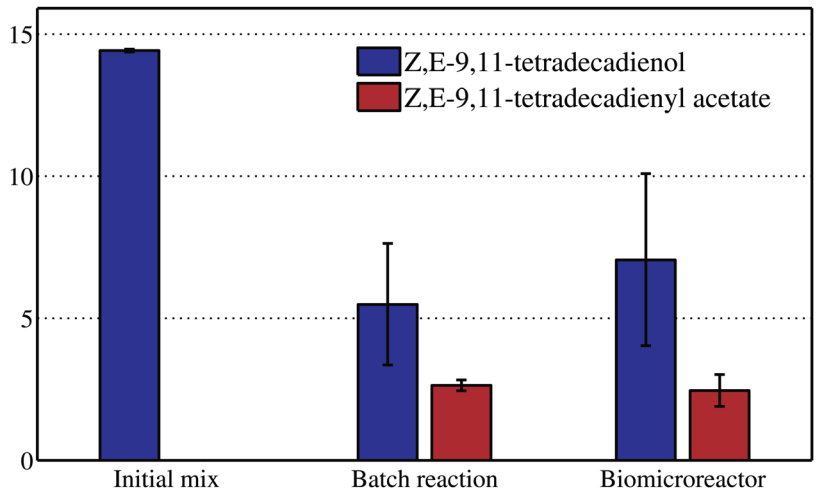

FIG. 9. Conversion of (*Z,E*)-9,11-tetradecadienol into (*Z,E*)-9,11-tetradienyl acetate in batch and after single passing through a biomicroreactor coated with PEM and containing *atf* immobilized on beads.

EGFP molecule is not adsorbed on a positively charged surface, this would mean that no interaction would be expected for the positively charged *atf* either.

However, in their work on adsorption of lysozyme at a model charged surface, Kubiak-Ossowska and Mulheran[36] argue that electrostatic interactions might not be sufficient to dominate protein adsorption. This opinion is confirmed by Müller and Paulik,[27] who state that adsorption is possible for negatively charged human serum albumin on negatively charged poly(vinylsulfate).[22] Accordingly, such interaction would occur between charged domains of the protein molecule and dissociated polyanion. Although the adsorption behavior of His_6-EGFP cannot be translated unconditionally on *atf*, it provides valuable information about adsorption on PEI terminated coating. The experimental results evidence that PEI/His_6-EGFP interactions are weak and reversible.

D. Biomicroreactor activity in comparison with batch activity

The reactions were conducted after thorough washings of the microreactor with buffer solution, indicating that the enzyme was successfully immobilized by coordination bonds to the agarose beads. Thus the PEI/DSS multilayer coating was proved inert towards the immobilized enzyme.

The results from these experiments are illustrated in Fig. 9 and show similar conversion in the biomicroreactor and in the batch. Considering the mean values for detected (*Z,E*)-9,11-tetradecadienol and (*Z,E*)-9,11-tetradienyl acetate from the batch and PEM coated microreactor, there is a loss of approximately 30% in each system, compared to the amount of (*Z,E*)-9,11-tetradecadienol in the initial mix. Despite the non-complete recovery, a working biomicroreactor was presented thus proving the functionality of the anchored five layers coating based on the PEI/DSS.

IV. CONCLUSIONS

In summary, a PEM coated silicon/glass microreactor has been developed to mimic the biosynthetic last step of the pheromone of *S. littoralis*. The PEI/DSS multilayer coating was able to mask the active sites on silicon surfaces, thus considerably reducing adsorption of the substrate and the pheromone. Equally important, the PEI terminated coating demonstrated inertness towards His_6-EGFP from which was presumed an identical lack of interaction with the His_6-*atf*. The PEI/DSS properties were affected by *p*H and time of deposition and therefore these parameters could be used to achieve the desired thickness and morphology of the coating.

Our findings would allow to optimize the infochemical pheromone synthesis using biomicroreactors. More generally, the explored PEI/DSS couple could be applied successfully as an anti-adsorption coating in a variety of silicon surfaces using polar substrates.

ACKNOWLEDGMENTS

The authors would like to acknowledge financial support for this project from the Sixth Framework Programme of the European Union through Information Society Technologies, FP6-IST 032275. We would like to thank Herbert Wormeester for his help with the ellipsometry measurements and Daniel Ebeling for his valuable contribution to the AFM studies. We thank Vinod Subramaniam for cordially providing us with the His_6-EGFP. Last but not least, we would like to thank Alexander Steinbüchel (Institut für Molekulare Mikrobiologie und Biotechnologie, Westfälische Wilhelms Universität, Münster) for kindly providing us with the expression vector pET23a containing the His_6-*atf*.

[1]L. Muñoz, G. Rosell, C. Quero, A. Guerrero, Physiol. Entomol. **33**, 275 (2008).
[2]M. Cole, J. Gardner, Z. Racz, S. Pathak, A. Guerrero, L. Muñoz, G. Carot, T. Pearce, and J. Challiss, *et al*., in *Sensors, 2009 IEEE* (IEEE, Washington, DC, 2010), pp. 1358–1361.
[3]S. Uthoff, T. Stoveken, N. Weber, K. Vosmann, E. Klein, R. Kalscheuer, and A. Steinbüchel, Appl. Environ. Microbiol. **71**, 790 (2005).
[4]J. Melin and S. R. Quake, Biophysics **36**, 313 (2007).
[5]D. Peterson, T. Rohr, F. Svec, J. Fréchet, Anal. Chem. **74**, 4081 (2002).
[6]K. Sakai-Kato, M. Kato, and T. Toyoóka, Anal. Chem. **75**, 388 (2003).
[7]J. Drott, K. Lindström, L. Rosengren, T. Laurell, J. Micromech. Microeng. **7**, 14 (1997).
[8]T. Honda, M. Miyazaki, H. Nakamura, and H. Maeda, Chem. Commun. **40**, 5062 (2005).
[9]G. Seong, J. Heo, and R.M. Crooks, Anal. Chem. **75**, 3161 (2003).
[10]H. Holmes and J. Kelevy, J. Phys. Chem. **32**, 1522 (1928).
[11]A. Dabrowski and V. Tertykh, *Adsorption on New and Modified Inorganic Solvents* (Elsevier Science, Amsterdam, The Netherlands, 1996).
[12]R. Iler, J. Colloid Interface Sci. **21**, 569 (1966).
[13]G. Decher, J. Hong, and J. Schmitt, Thin Solid Films **210**, 831 (1996).
[14]H. Kim and M. Urban, Langmuir **14**, 7235 (1998).
[15]A. Wang, J. Xu, Q. Zhang, and H. Chen, Talanta **69**, 210 (2006).
[16]R. Liang, G. Gan, and J. Qiu, J. Sep. Sci. **31**, 2860 (2008).
[17]W. Bauer, M. Fischlechner, C. Abell, and W. Huck, Lab Chip **10**, 1814 (2010).
[18]N. Hoogeveen, M. Cohen-Stuart, G. Fleer, and M. Bömer, Langmuir **12**, 3675 (1996).
[19]S. Shiratori and M. Rubner, Macromolecules **33**, 4213 (2000).
[20]P. Bieker and M. Schönhoff, Macromolecules **43**, 5052 (2010).
[21]M. Müller, T. Rieser, K. Lunkwitz, and J. Meier-Haack, Macromol. Rapid Commun. **20**, 607 (1999).
[22]M. Müller, T. Rieser, P. Dubin, and K. Lunkwitz, Macromol. Rapid Commun. **22**, 390 (2001).
[23]G. Lindquist and R. Stratton, J. Colloid Interface Sci. **55**, 45 (1976).
[24]G. Koper, R. van Duijvenbode, D. Stam, U. Steuerle, and M. Borkovec, Macromolecules **36**, 2500 (2003).
[25]R. Mészáros, I. Varga, and T. Gilányi, Langmuir **20**, 5026 (2004).
[26]R. Mészáros, L. Thompson, M. Bos, and P. de Groot, Langmuir **18**, 6164 (2002).
[27]M. Müller and S. Paulik, Macromol. Symp. **265**(1), 77 (2007).
[28]J. Yakovleva, R. Davidsson, A. Lobanova, M. Bengtsson, S. Eremin, T. Laurell, and J. Emnéus, Anal. Chem. **74**, 2994 (2002).
[29]S. Chang, K. Gooding, and F. Regnier, J. Chromatogr. A **120**, 321 (1976).
[30]W. Bula, W. Verboom, D. Reinhoudt, and H. J. G. E. Gardeniers, Lab Chip **7**, 1717 (2007).
[31]G. Fleer, *Polymers at Interfaces* (Chapman & Hall, London, 1993).
[32]T. Lee and A. Feig, RNA **14**, 514 (2008).
[33]B. Derjaguin and L. Landau, Acta Physicochim. USSS **14**, 633 (1941).
[34]E. Verwey and J. Overbeek, *Theory of the Stability of Lyophobic Colloids* (Elsevier, New York, 1948).
[35]T. Stoveken, R. Kalascheuer, U. Malkus, R. Reichelt, and A. Steinbuchel, J. Bacteriol. **187**, 1369 (2005).
[36]K. Kubiak-Ossowska and P. Mulheran, Langmuir **26**, 7690 (2010).